Near Acoustic Field and Shock Structure of Rectangular Supersonic Jets

E. Gutmark,* K. C. Schadow,† and C. J. Bicker‡
Naval Weapons Center, China Lake, California, 93555

An underexpanded supersonic rectangular jet is studied experimentally at a pressure ratio range of 1–15. The shock-cell and shear-layer structure variation with the pressure ratio is shown to be related to the near-field pressure fluctuations. Near the sonic, fully adapted velocity, the jet is fully symmetric. An abrupt change to a flapping mode occurs at a low Mach number, causing a large increase in the spreading rate, which is also related to the appearance of an upstream propagating screech component. This behavior is observed at the minor axis plane, whereas the other plane remains symmetric. As the pressure ratio is further increased, the jet growth is decreased concurrently with the reduction of the upstream propagating pressure component. At the same time, the broadband near-field pressure fluctuations are enhanced. At the highest pressure ratio measured, the jet becomes quasisymmetric, with a dominant helical screech tone and a very large spreading rate at both axis planes.

Introduction

JET flows are an important part of various mixing devices and thrust-producing propulsion systems. Different methods have been studied to increase their entrainment rates to achieve better mixing and to augment thrust. A passive technique of increasing entrainment was found by using a small-aspect-ratio elliptic jet.[1] It was shown that the self-induction of the asymmetric coherent structures increased the amount of ambient fluid engulfed by this jet. Schadow et al.[2] studied elliptic jets in a high Reynolds number range with reactive exothermic flow and showed that higher entrainment, as well as better small-scale mixing, increased the temperature of the reacting jet.

One of the special features of asymmetric or three-dimensional jets (elliptic or rectangular) was the axis switching. Earlier work done with these jets[3] showed that they spread in the minor axis plane more than in the major axis plane, resulting in a crossover point at which the jet became locally quasiaxisymmetric. Downstream of this point the major axis became the minor one, and vice versa. The axial location of this crossover point was found to be proportional to the initial aspect ratio of the jet's nozzle. Krothapalli et al.[4] extended their study[3] of large-aspect-ratio ($AR = 10$) rectangular jets to supersonic speeds, studying the structure of underexpanded jets having the same aspect ratio. They found that the spreading rate at the minor axis side grew even further, relative to subsonic flow, in the presence of shocks in the jet's core. Maximum growth was obtained at a nozzle pressure ratio of 3.8, corresponding to a Mach number of $M = 1.5$, based on fully expanded isentropic flow equations. At higher pressure ratios ($M = 1.8$), the spreading rate decreased but was still higher than in the subsonic jet.

A possible explanation for the high spreading rate of underexpanded jets could be related to the interaction between the expansion/compression waves and the jet shear layer.[5] Measurements done in our laboratory with underexpanded supersonic jets[6] showed irregular change of the jet spreading rate with the Mach number. This behavior was attributed to the establishment of an acoustic feedback formed by sound waves that were generated in the downstream section of the jet by shock/shear-layer structures interaction and that then propagated upstream to force the initial shear layer at the nozzle lip to generate new structures in the shear layer.

The relation between the shear-layer structures and the sound field generated by the jet was established in low and high Reynolds number jets. Seiner[7] concluded, in a review of the advances in research of high-speed jet aeroacoustics, that there is ample evidence to show that large-scale coherent structures are an important source of jet noise production. Even the screech tone produced in an imperfectly expanded supersonic jet was shown to be the same as the most amplified instability waves in the flow.[7] Theoretical models that were based on these ideas[8] were able to predict the near- and far-field acoustics of a supersonic plume. The interaction between the jet flow structures and the acoustics is especially important in a ducted flow configuration (as in a combustor) when the interaction between the flow and the duct acoustics can modify the flow development.[9] This interaction can occur between multiple acoustic modes and jet modes.

In contradistinction to plane shear layers, jets have complex azimuthal mode structure, especially when the jet is noncircular. The flow characteristics and noise of noncircular jets are not covered extensively in the literature. Krothapalli et al.[3,4] studied rectangular jets of large aspect ratio, in the range of $AR = 6$–13 (quasi-two-dimensional) and found that the noise of these jets when operated in choked conditions is dominated by discrete frequencies—the screech tones—similar to the circular jet. Tam[10] developed a simple linear shock-cell model to solve the shock-cell structure of a rectangular and elliptic jet. He obtained good agreement with experimental data in predicting the shock-cell spacing and the screech frequency for large-aspect-ratio jets in a range of Mach numbers between 1.15 and 1.8.

Gutmark et al.[11,12] studied the relation between the jet flow structure and near-field acoustics in circular and small-aspect-ratio elliptic jets. They showed that the higher spreading rate of the underexpanded, $AR = 3{:}1$ elliptic jet is associated with the generation of upstream propagating acoustic component. This component appeared in the flow when the jet mode switched from axisymmetric to flapping (in a noncircular jet) or helical mode (in a circular jet).

The present work describes the structure of a small-aspect-ratio ($AR = 3$) rectangular jet operated at choked conditions in a wide range of Mach numbers. The shock structure is visual-

Received May 1989; revision received Aug. 1989.

*Research Scientist, Research Department. Member AIAA.
†Supervisory General Engineer, Research Department.
‡Computer Engineer, Research Department.

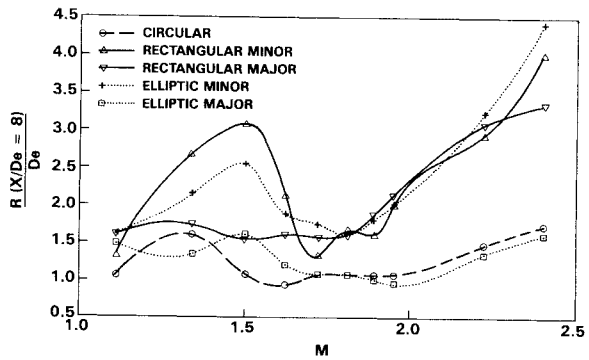

Fig. 1 Variation of the circular, rectangular, and elliptic supersonic jets width with Mach number at $x/D_e = 8$.

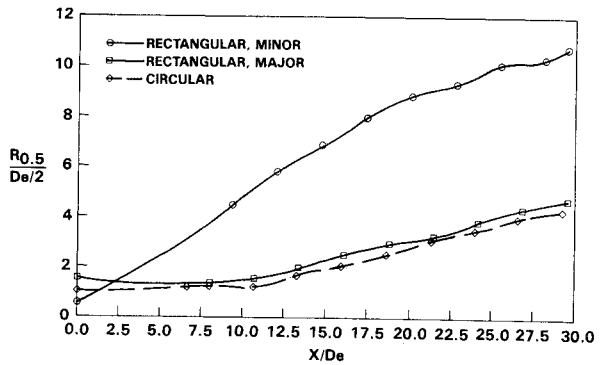

Fig. 2 Spreading rate of the circular and rectangular supersonic jets at $M = 1.5$.

ized using Schlieren spark photograph. The shock-cell spacing and screech frequencies are compared with Tam's theory. The near acoustic field is measured for the different conditions, including the distribution of the various frequency components. The mode structure of the jet is studied as a function of the Mach number.

Experimental Arrangement

A high-pressure blowdown air supply system was used to produce the jet. The jet system consisted of a cylindrical settling chamber, 24.1-cm long and 10.8 cm in diameter. The nozzle section was attached to the converging section of the settling chamber and was 6.4 cm long. The area ratio between the settling chamber and the nozzle's outlet area was 32. Three shapes of nozzles were studied: circular, rectangular, and elliptic. The circular nozzle diameter D and the equivalent diameter D_e of the noncircular nozzles were 1.9 cm. The aspect ratio of the rectangular nozzle AR was 3:1. The measurements were carried out for two conditions: 1) a fully expanded jet with sonic velocity at the exit and 2) an underexpanded jet in a Mach number M range of 1-2.4.

Spark Schlieren photography was used to obtain instantaneous flow visualization of the jets, revealing both the shock structure and the small-scale turbulence. Schlieren pictures with longer exposure times were used to visualize the variation of the shock structures in the different planes of the noncircular nozzle configurations.

Hot-wire anemometry was used to determine the spreading rate of the jet for the various Mach numbers studied. A 3.175-mm B&K microphone was used for near-field pressure fluctuations measurement. The microphone has an open circuit frequency response of up to 140 kHz according to manufacturer's specifications. It was mounted on a computer-controlled precise traverse mechanism, enabling movement in all three axes. A typical measurement grid included 300 points covering the entire near field of the jet from a normalized axial distance of $x/D = 5$ behind the nozzle exit to 20 diameters downstream from the exit and to a radial distance (r) of $11D$ from the jet edge The microphone was calibrated using a B&K calibration type 4220 piston phone.

Spectral analysis was performed in many measurement points to follow the jet instability characteristics and to determine the dominant acoustic components in the near field. The microphone and hot-wire calibration, data acquisition and analysis were done using a VAX-750 minicomputer.

Results and Discussion

Axisymmetric and elongated underexpanded jets typically exhibit varying flow structures and evolution patterns near the sonic velocity and at higher Mach numbers. Different facets of this behavior are discussed in this paper.

A. Spreading Rate

Starting with the spreading rate, Fig. 1 shows the visual jet width 8 diameters (or equivalent diameters) downstream of the

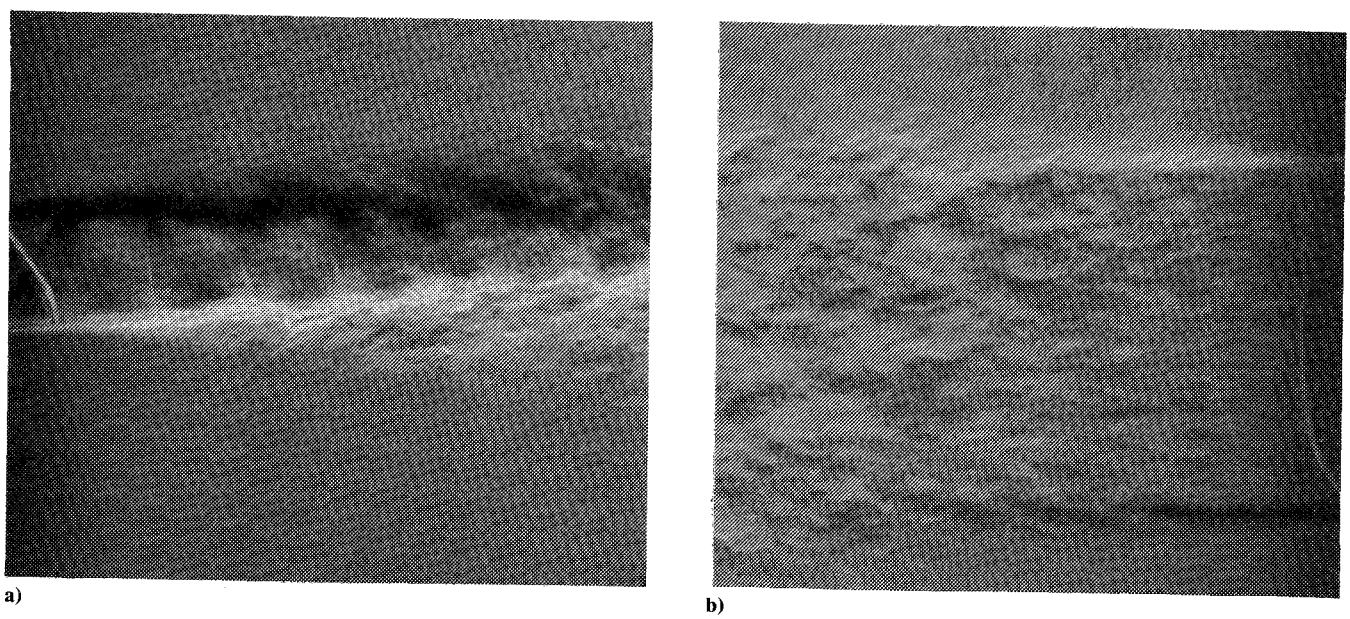

a) b)

Fig. 3 Schlieren spark photograph of the symmetric mode of the rectangular jet for $M = 1.1$ at a) the minor axis plane and b) the major axis plane.

nozzle, obtained from Schlieren spark photographs. The circular jet shows a peak spread in the range of $1 < M < 1.5$. Similar but higher peaks are observed in the elliptic and rectangular spread at the minor axis plane, in the range of $1 < M < 1.7$. After a dip, which occurs at $1.6 < M < 1.8$, all jets show increased spread with Mach number, at different rates. The rectangular jet at both planes and the elliptic jet only at the minor axis plane reach a width at $M = 2.4$, which is even higher than the first peak. Gutmark et al.[11,12] showed that the peak at the lower Mach number range is related to the mode switching of the circular and elliptic jets. It is shown in the present paper that the rectangular jet exhibits similar behavior at that range. However, the two elongated jets have very different behavior at the higher Mach number; the rectangular jet spreads at both axis planes at a similar rate, whereas the elliptic jet switches axes, and the spread occurs only at the minor axis plane, whereas the major axis side grows slowly like the circular jet. These differences are also seen in the near-field pressure, as discussed later.

The large difference between the rectangular jet spreading rate at the major axis and minor axis at the peak location corresponding to $M = 1.5$ was also measured using a hot-wire anemometer and is compared to a circular jet in Fig. 2. The rectangular jet spreads at the major axis plane at a rate similar to that of the circular jet whereas, at the minor axis plane, the high spread results in axes switching at $x/D_e = 2.5$ from the jet exit. Similar results were measured for an elliptic jet at $M = 1.3$ and 1.4.[11]

B. Flow Visualization

The variation in the jet structure corresponding to the different Mach numbers is visualized using spark Schlieren photography. Figures 3a and 3b show two views of the rectangular jet at $M = 1.1$, of the minor and major sides, respectively. The shock-cell pattern and the shear layers on both sides are symmetric, with a spreading angle similar to a subsonic jet. As the Mach number is increased to the range corresponding to the increased jet spread, $M = 1.34$, as show in Fig. 4, the structure becomes very different. Figures 4a and 4b show two instantaneous pictures of the minor axis plane view of the jet during its flapping motion when, in 4a, it bends to the left, shedding the first vortex to this side, whereas, in 4b, it bends and sheds the initial vortex to the right. The antisymmetric structure of the shear layers is evident. The major axis plane view (Fig. 4c) remains with a symmetrical structure. The maximum spread is reached at $M = 1.5$ (Fig. 5), where the larger field of view in the photograph shows both the flapping "braided" structure and the large subsequent spreading rate further downstream. Concurrently, the major axis plane has a symmetric appearance with low spread.

At the higher Mach number range of $1.7 < M < 1.9$, the antisymmetric structures are no longer obvious in the jet flow, and the spreading rate decreases as well. As the flow speed is further increased, the jet spread grows gradually. At the highest Mach number measured ($M = 2.4$), the large width of the jet is regained (Fig. 6), this time at both sides of the jet. The "barrel" shock is clearly visualized downstream of the nozzle, as well as strong propagating sound waves, from the jet circumference, especially at the minor axis plane.

C. Shock-Cell Structure and Screech Tone

The shock-cell structure of the different jets was measured for different Mach numbers. The shock-cell structure, which starts, for the lower Mach numbers, as a series of oblique shocks and expansion fans impinging on, and reflecting from, the jet shear layers, changes its characteristics for higher Mach numbers ($M > 1.8$) when a normal shock is formed. The vari-

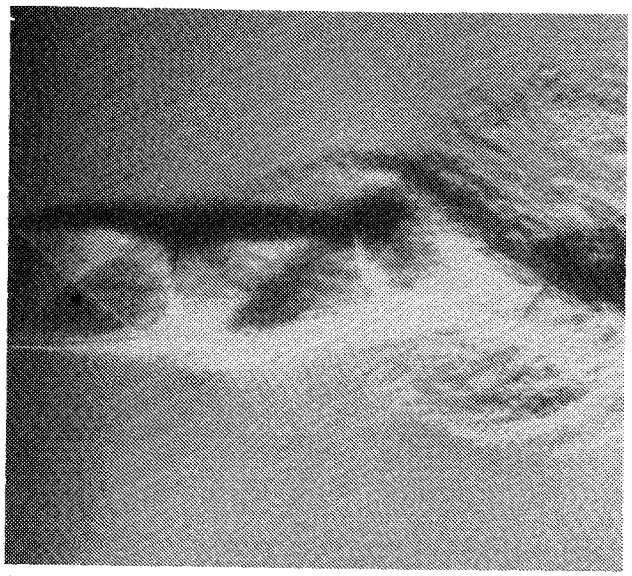

a)

b)

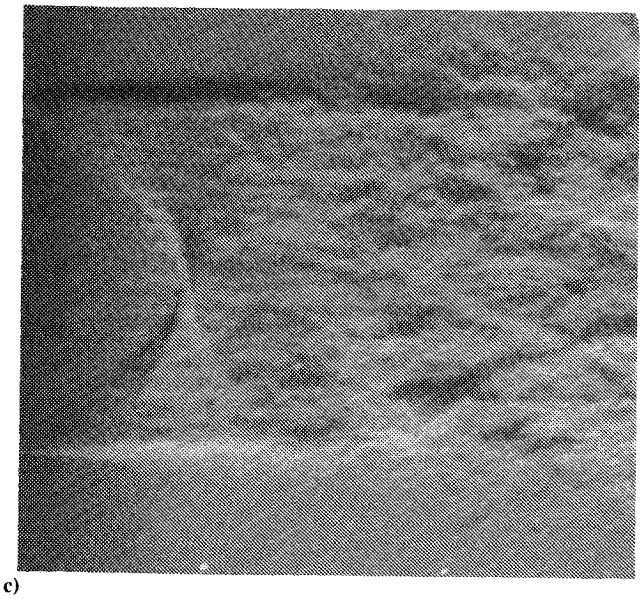

c)

Fig. 4 Schlieren spark photograph of the flapping mode of the rectangular jet at $M = 1.34$: a) minor axis plane, flapping to one side; b) minor axis plane, flapping to the other side; and c) major axis plane.

ation of the average shock-cell length with the jet fully expanded Mach number [given here as the function of the shock-cell parameter, $\beta=(M^2-1)^{0.5}$] for a circular, elliptic, and rectangular jet is shown in Fig. 7. It was shown by Seiner[7] that the normalized shock-cell spacing L/D, where D is the jet exit diameter (or equivalent diameter for a noncircular jet) varies with the jet Mach number M as $L/D=a(M^2-1)^{b/2}$. Similar behavior is obtained for the noncircular tests, with the slope of the noncircular jets (elliptic $b=1.31$ and rectangular $b=1.57$) larger than that of the circular jet ($b=1.15$).

Tam[10] obtained good agreement with experimental results, calculating the variation of the shock-cell spacing with the jet Mach number, using a linear shock-cell model. His comparison was done with available data for high-aspect-ratio rectangular jets that were quasi-two dimensional. Figure 8 shows a comparison of the same theory with the present data for a rectangular jet with an aspect ratio of 3. The shock-cell spacing is normalized by the rectangular minor axis width h. Both the predicted and the measured curves fall below those of a large aspect ratio, with excellent agreement especially for $M \leq 1.7$. For higher Mach numbers, where normal shocks appear in the jet core, the trend is still in agreement with the experiments, but the data deviate more from the prediction.

Using the same model, Tam[10] predicted also the variation of the screech tone Strouhal number with the jet Mach number. Again, the comparison was limited to high-aspect-ratio jets. Figure 9 adds the present data for the small-aspect-ratio rectangular jet. The frequency is normalized by h and the exit velocity U_O. The theory does not show a significant change between the small- and large-aspect-ratio cases. The experimental results also overlay the earlier large-aspect-ratio results. The agreement between the measured and calculated results is very good except for the lower range of Mach numbers.

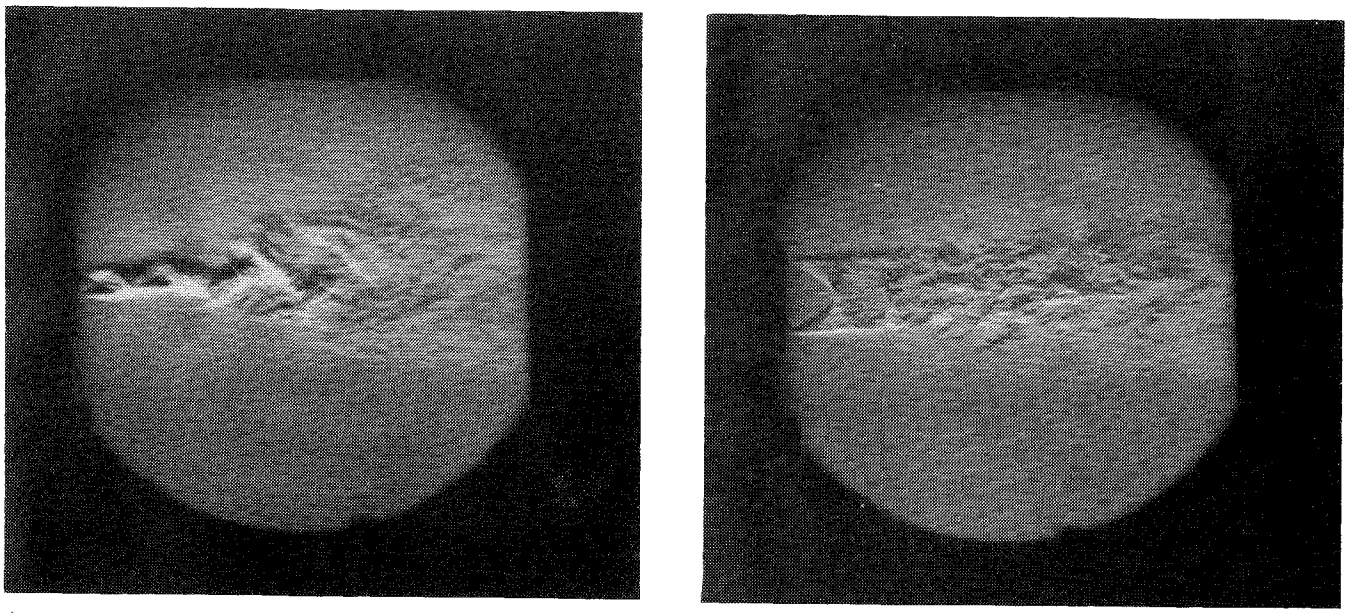

a) b)

Fig. 5 Schlieren spark photograph of the flapping mode of the rectangular jet at $M = 1.5$: a) minor axis plane and b) major axis plane.

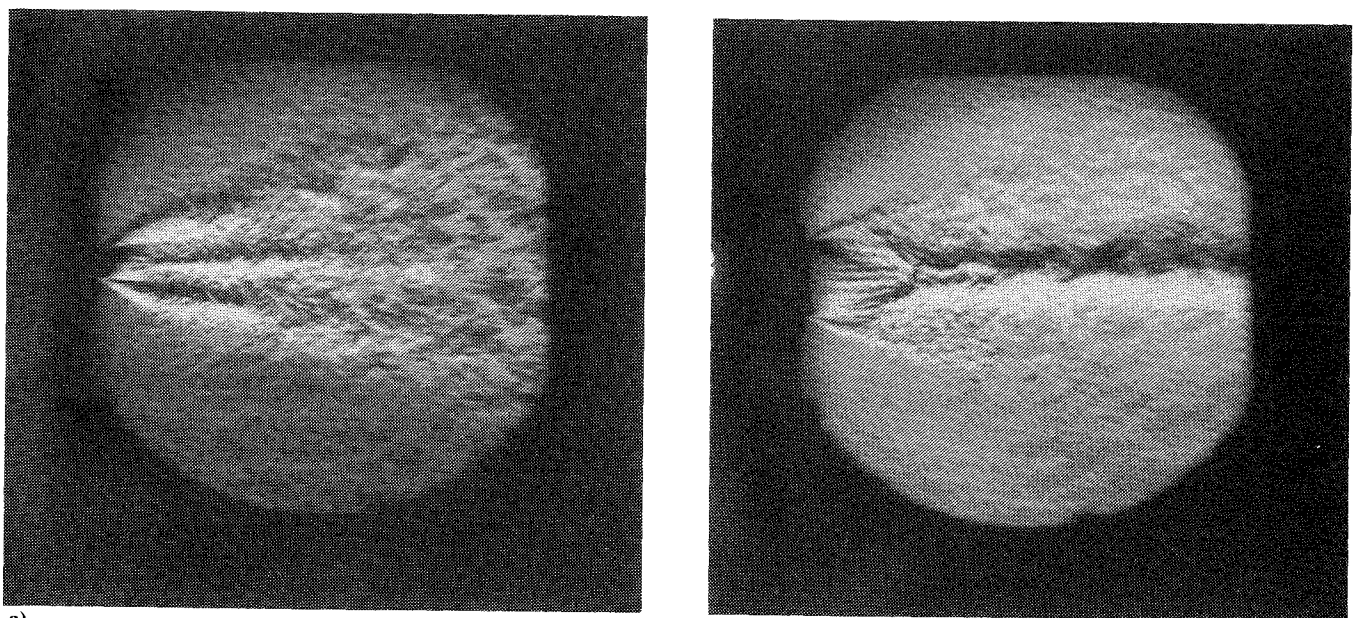

a) b)

Fig. 6 Schlieren spark photograph of the rectangular jet at $M = 2.4$: a) minor axis plane and b) major axis plane.

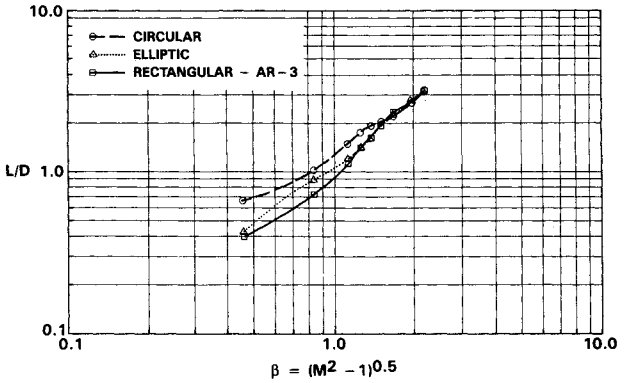

Fig. 7 Variation in the shock-cell spacing with the jet Mach number parameter β.

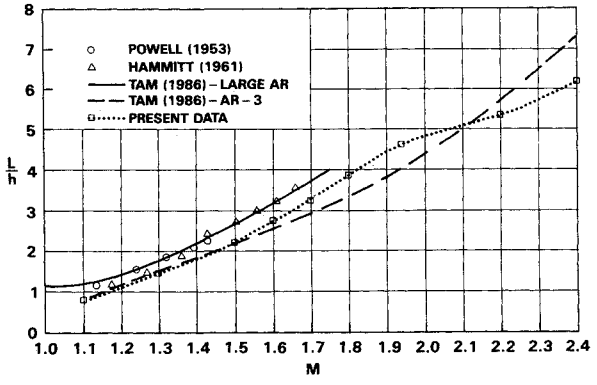

Fig. 8 Variation in the shock-cell spacing with jet Mach number for small and large $\mathcal{R}$; comparison of measurements and theory.

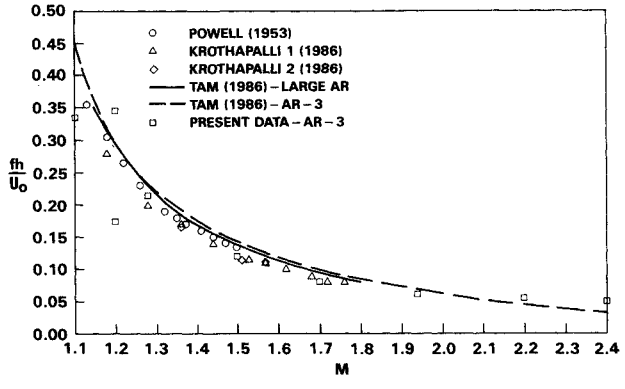

Fig. 9 Variation of the screech tone Strouhal number as a function of jet Mach number; comparison of measurements and theory.

D. Mode Switching

The flow visualization data described in subsection B indicate that a change in the jet structure occurs as the Mach number varies. The switch from symmetric to flapping mode was further studied by placing high-frequency response microphones around the jet circumference and analyzing the spectral peak frequencies and spatial phase relation between them. Figures 10 and 11 show the cross spectra ($E(f)$ and phase angle variation with frequency for the near-field pressure fluctuations measured across the minor and major axis planes, respectively, for $M=1.08$. The frequency with the highest energy level corresponds to $St=(f\cdot D_e)/(a\cdot M)=1.01$ (where f is the frequency; D_e, equivalent diameter; and a the speed of sound) and its subharmonic at the major axis plane. The phase angle of the peak frequency at the minor axis plane was 70 deg and was 4.5 deg at the major axis plane. These phase angles correspond to a nearly symmetric structure on both axis planes. The switch to a flapping mode is very abrupt at $M=1.15$. It is different than the similar phenomenon observed earlier in a circular jet, where the transition is gradual and occurs over a relatively wider range of Mach numbers.[12] The cross spectra and phase angle distribution following the transition, for $M=1.34$, are shown in Figs. 12 and 13 for the minor and major axis planes. The dominant spectral peak for this condition is at $St=0.34$. Its amplitude is more than two orders of magnitude larger at the minor axis plane than at the major axis plane. The phase angle at the former is 160 deg, corresponding to a flapping motion of the jet at this plane where, at the major, the angle is 13 deg, which is related to the symmetric behavior of the jet at this plane. The first harmonic ($St=0.68$) is nearly symmetric, in both sides of the jet. For higher Mach numbers, $M=1.95$, in Figs. 14 and 15, the phase angle at both planes becomes nearly 180 deg, indicating transition to a helical mode as the jet geometry becomes quasiaxisymmetric. The peak frequency for this condition is at $St=0.145$, and its amplitude at the major axis plane is larger than at the minor. Similar variation of the jet mode structure was observed for the elliptic supersonic underexpanded jet.

E. Near-Field Pressure Fluctuations

Mean flow measurements[6] and stability theory analysis[13] showed that the deviation of the jet from symmetry, either by

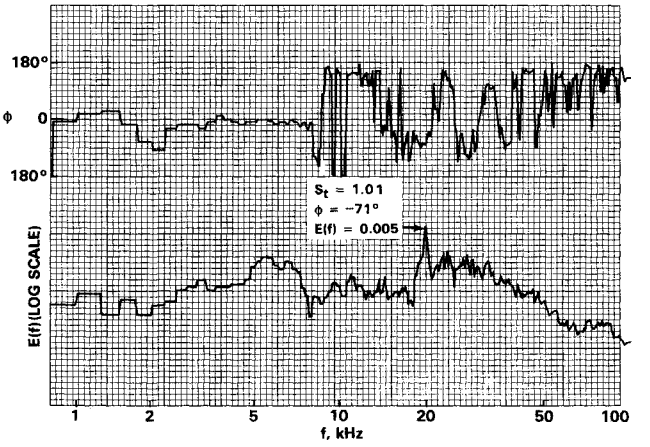

Fig. 10 Cross spectrum and relative phase of near-field pressure fluctuations at opposite jet boundaries, minor axis plane, $M=1.08$ ($x/D_e=0.67$, $r/D_e=\pm 0.94$).

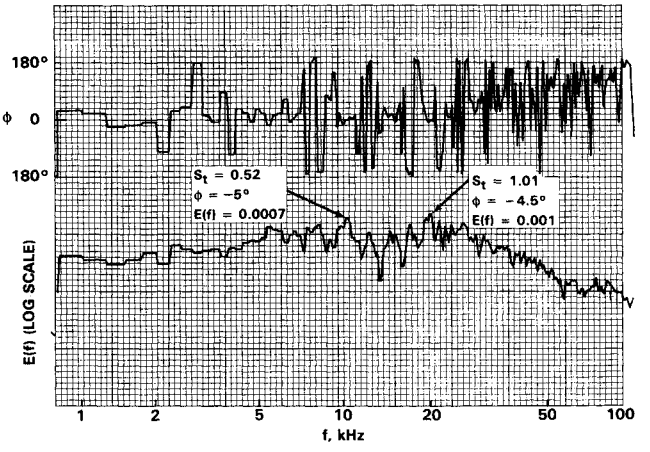

Fig. 11 Cross spectrum and relative phase of near-field pressure fluctuations at opposite jet boundaries, major axis plane, $M=1.08$ ($x/D_e=0.67$, $r/D_e=\pm 0.94$).

eccentricity, as in the elliptic and rectangular jet, or by introducing sharp corners, as in rectangular, triangular or square jets, causes changes in the jet's behavior at the different regions around its circumference. These changes are related to the local radius of curvature of the nozzle edge and to the boundary-layer thickness at this location, and they affect the flow instability characteristics, the evolution of the large-scale structures, the shock-cell geometry, and the eventual jet noise characteristics.

Measurements of the near pressure field, made at the minor and major planes of the rectangular jet, showed a significant difference in the pressure field between those regions. The level of pressure fluctuations at the minor plane side (Fig. 16) is much higher than at the major plane side (Fig. 17). The pattern is also different, exhibiting a double lobe pattern at the minor plane side, where one lobe propagates upstream of the jet exit and one downstream of the exit in a normal direction to the jet flow. At the major plane section, only the latter pattern is observed. It is shown, in the following discussion, that the upstream propagating lobe is related to the strongest screech frequency component, whereas the downstream part is related to a combination of its harmonics. This behavior is also different at the major plane, where no upstream propagating component is present.

For jet Mach numbers larger than 1.7, the differences between the two planes are reduced and, as the jet becomes quasiaxisymmetric, the near-field pressure fluctuation contours are similar. For example, at $M=2.2$ (Figs. 18 and 19), the minor axis plane still has slighy higher intensity than the major side, but their patterns are similar. There is no significant upstream lobe as for the lower Mach number range. At the minor axis plane (Fig. 18), the local maxima due to the first three shock-cell structures are evident at the jet boundary. This behavior is different from that of the elliptic jet[12] which, at the same Mach number range, had a significantly stronger acoustic field at the major axis relative to the minor axis plane.

The contribution of each spectral peak component to the near-field pressure was studied by mapping the amplitude of each frequency component separately in the entire near field. The results for the minor axis plane of the $M=1.35$ jet are shown in Fig. 20 for the fundamental frequency ($St=0.34$) and its first harmonic ($St=0.68$) and Fig. 21 for the second ($St=1.02$) and third harmonics ($St=1.36$). The antisymmetric fundamental frequency is dominant only upstream of the nozzle exit, whereas the first harmonic, which was shown to be symmetric (Fig. 12), is dominant downstream of the exit, normal to the jet. Its peak level amplitude is an order of magnitude lower than the fundamental frequency. The higher harmonics are even lower in amplitude; however, each frequency component has its own "territory," where it is dominant. The combination of all these harmonics constitutes the downstream lobe of the near-field pressure. The third harmonic,

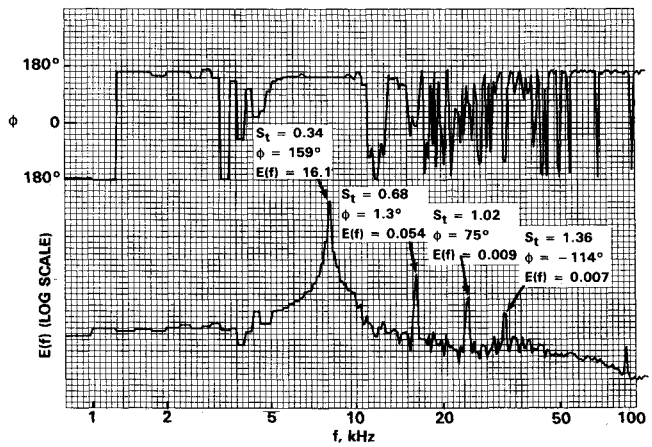

Fig. 12 Cross spectrum and relative phase of near-field pressure fluctuations at opposite jet boundaries, minor axis plane, $M=1.34$ ($x/D_e=0.67$, $r/D_e=\pm 0.94$).

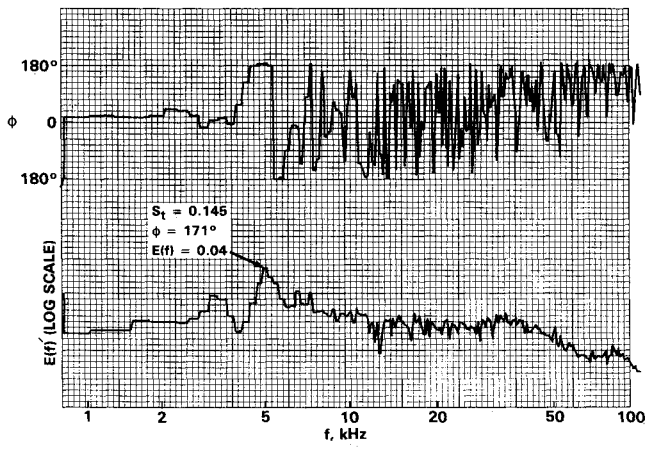

Fig. 14 Cross spectrum and relative phase of near-field pressure fluctuations at opposite jet boundaries, minor axis plane, $M=1.95$ ($x/D_e=0.67$, $r/D_e=\pm 0.94$).

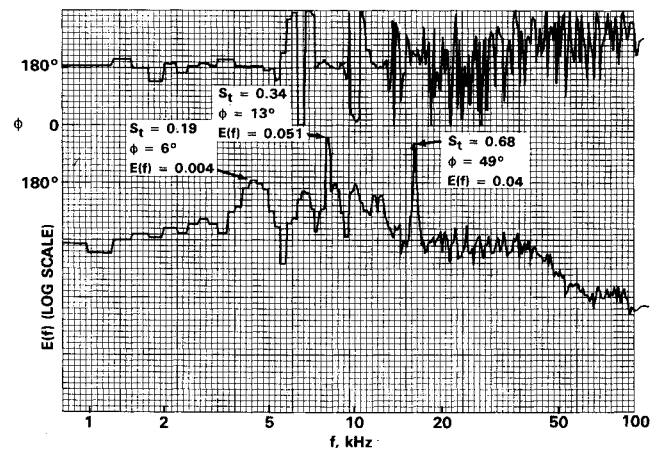

Fig. 13 Cross spectrum and relative phase of near-field pressure fluctuations at opposite jet boundaries, major axis plane, $M=1.34$ ($x/D_e=0.67$, $r/D_e=\pm 0.94$).

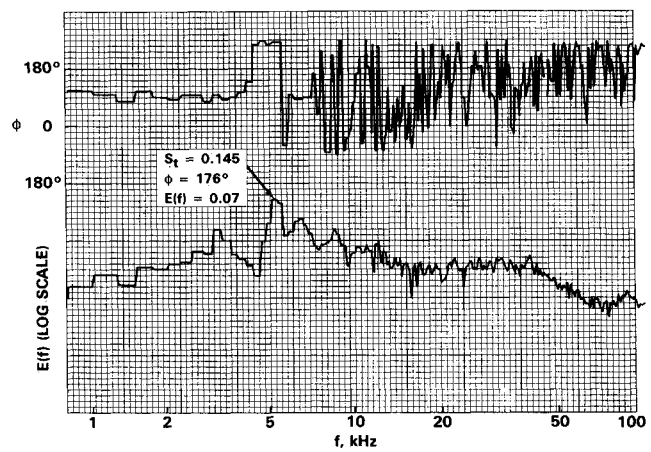

Fig. 15 Cross spectrum and relative phase of near-field pressure fluctuations at opposite jet boundaries, major axis plane, $M=1.95$ ($x/D_e=0.67$, $r/D_e=\pm 0.94$).

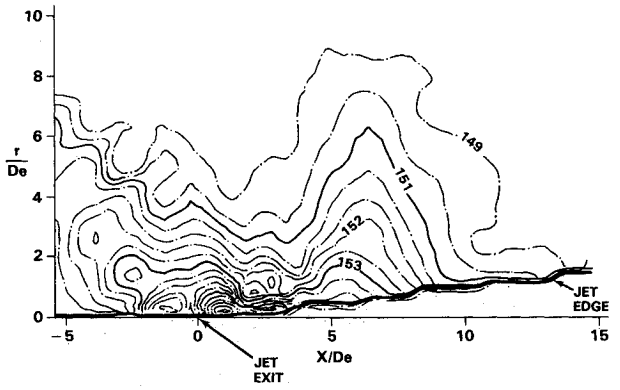

Fig. 16 Contours of the near-field pressure fluctuations of the rectangular jet, minor axis plane, $M=1.5$; contour lines are sound pressure level in decibels.

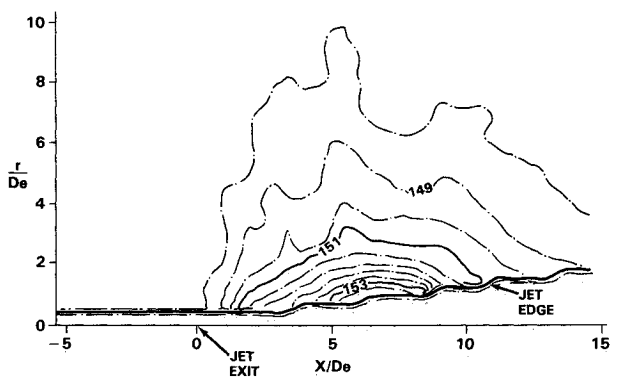

Fig. 17 Contours of the near-field pressure fluctuations of the rectangular jet, major axis plane, $M=1.5$; contour lines are sound pressure level in decibels.

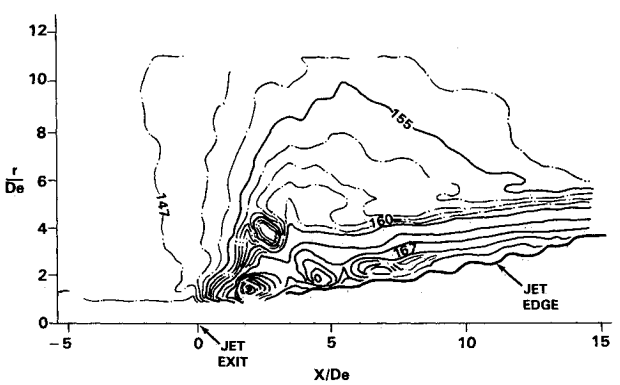

Fig. 18 Contours of the near-field pressure fluctuations of the rectangular jet, minor axis plane, $M=2.2$; contour lines are sound pressure level in decibels.

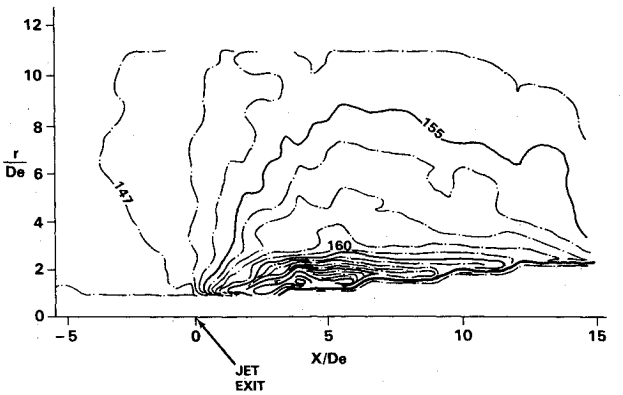

Fig. 19 Contours of the near-field pressure fluctuations of the rectangular jet, major axis plane, $M=2.2$; contour lines are sound pressure level in decibels.

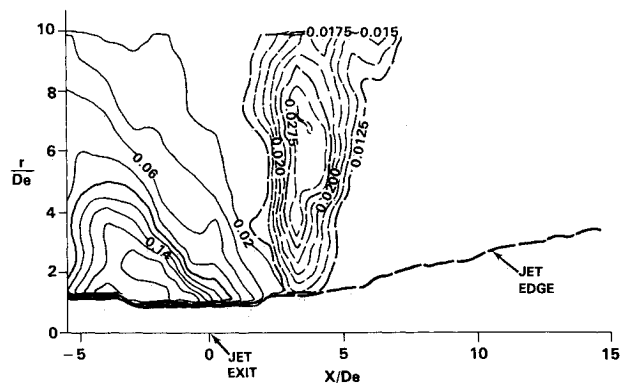

Fig. 20 Contours of equal amplitude of the fundamental dominant frequency ($St=0.34$), —, and first harmonic ($St=0.68$), ----, of the near-field pressure fluctuations at $M=1.35$; contour numbers indicate relative amplitude values.

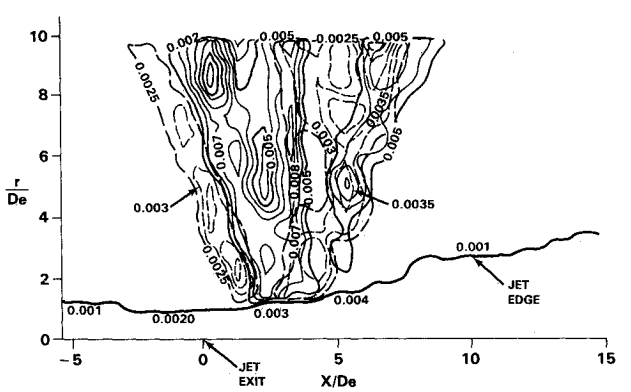

Fig. 21 Contours of equal amplitude of the second harmonic ($St=1.02$), —, and the third harmonic ($St=1.36$), ----, of the near-field pressure fluctuations at $M=1.35$; contour numbers indicate relative amplitude values.

which had a relatively high phase angle across the minor side of the jet ($\phi=114$ deg), has an upstream-directed component of the near-field pressure fluctuations. The same components at the major axis plane had very low amplitude and were evenly distributed along the jet edge downstream of the jet exit. For the higher Mach number, $M=1.72$, corresponding to asymmetric near-field pressure at both axis planes, the screech component is dominant in both planes upstream of the exit, as the helical (or flapping) modes typically behave. However, the main energy of the pressure fluctuations is concentrated downstream of the nozzle and is associated with a broad band of frequencies.

Summary and Conclusions

A significant variation of the supersonic underexpanded rectangular jet is observed from near-sonic velocity to higher Mach numbers. The changes in the jet structure and flowfield result in corresponding variation of the near-field pressure. Initially, near sonic (fully adapted) conditions, the jet is axisymmetric in both minor and major axis planes. Its spreading rate is similar to the subsonic rectangular jet. A sudden transition to an asymmetric flapping mode at the minor axis plane results in a large increase in the spreading rate at this plane. The amplitude of the near-field pressure fluctuations is high as well at this side. The major axis plane remains symmetric, with low

spread and low pressure fluctuations. Previous measurements showed that the turbulent flow fluctuations at the minor axis plane are amplified at a higher rate as a result of the energy transferred to them from the mean velocity field. Similar behavior was observed for circular and elliptic jets; however, the mode switching in the former is gradual and not as abrupt as in the noncircular jets.

The flapping mode is also characterized by a dual pattern of the near-field fluctuating pressure. The highest screech component is propagating in the upstream direction and is found to dominate the region upstream of the jet exit. The combination of this behavior and the larger spreading rate supports the theory of the feedback between the screech tone and the mean flow, which suggests that the upstream propagating acoustic components excite disturbances at the initial shear layer of the jet. These disturbances are subsequently amplified in the shear layer, enhance its growth rate, and interact with the shock structures to produce a more intense acoustic field. Similar analysis that was used to predict shock-cell spacing and screech frequencies gives good agreement with the present experimental results.

The large-amplitude flapping of the jet is reduced as the Mach number is further increased, resulting in a lower spreading rate. The near-field pressure fluctuations are increased; however, the upstream propagating screech component is reduced while the broadband component is enhanced. As the Mach number is further increased, the jet spreading rate at both axes is enhanced. The behavior at this range is very different from that of the circular and even the elliptic jets. The former's spreading rate doesn't change significantly except in the region close to the nozzle as a result of the rapid external expansion. The elliptic jet exhibits behavior similar to the rectangular jet at the minor axis plane, but the growth rate at its major axis is similar to the circular jet. This difference between the two noncircular jets is also reflected in their near-field pressure patterns. The major axis plane of the elliptic jet becomes dominant in acoustic radiation whereas, in the rectangular jet, the two planes become similar, with a slightly stronger acoustic radiation at the minor axis plane.

The differences between the two jets are due mainly to the corner flow regions affecting the stability characteristics of the jet and its evolution. The effect of sharp corners on supersonic jet evolution is currently being studied in our laboratory.

References

[1]Ho, C. M., and Gutmark, E., "Vortex Induction and Mass Entrainment in a Small Aspect Ratio Elliptic Jet," *Journal of Fluid Mechanics*, Vol. 179, 1987, pp. 383–405.

[2]Schadow, K. C., Wilson, K. J., Lee, M. J., and Gutmark, E., "Enhancement of Mixing in Reacting Fuel-Rich Plumes Issued from Elliptical Nozzles," *Journal of Propulsion and Power*, Vol. 3, March–April 1987, pp. 145–149.

[3]Krothapalli, A., Baganoff, D., and Karamcheti, K., "On the Mixing of a Rectangular Jet," *Journal of Fluid Mechanics*, Vol. 107, 1981, pp. 201–220.

[4]Krothapalli, A, Hsia, Y., Baganoff, D., and Karamcheti, K., "On the Structure of an Underexpanded Rectangular Jet," Stanford Univ., Stanford, CA, AIAA TR-47, July 1982.

[5]Glass, D. R., "Effects of Acoustic Feedback on the Spread and Decay of Supersonic Jets," *AIAA Journal*, Vol. 6, Oct. 1968, pp. 1890–1897.

[6]Gutmark, E., Schadow, K. C., and Wilson, K. J., "Noncircular Jet Dynamics in Supersonic Combustion," AIAA Paper 87-1878, 1987.

[7]Seiner, M., "Advances in High Speed Jet Aeroacoustics," AIAA Paper 84-2275, 1984.

[8]Tam, C. K. W., and Burton, D. E., "Sound Generated by Instability Waves of Supersonic Flows," *Journal of Fluid Mechanics*, Vol. 138, 1984, pp. 249–295.

[9]Schadow, K. C, Wilson, K. J., and Gutmark, E., "Characterization of Large-Scale Structures in a Forced Ducted Flow with Dump," *AIAA Journal*, Vol. 25, Sept. 1987, pp. 1164–1170.

[10]Tam, C. K. W., "On the Screech Tones of Supersonic Rectangular Jets," AIAA Paper 86-1866, 1986.

[11]Gutmark, E., Schadow, K. C., Wilson, K. J., and Bicker, C. J., "Acoustic Radiation and Flow Instabilities in Low Supersonic Circular and Elliptic Jets," *Physics of Fluids*, Vol. 31, Sept. 1988, pp. 2524–2532.

[12]Gutmark, E., Schadow, K. C., and Bicker, C. J., "Mode Switching in Supersonic Circular Jets," *Physics of Fluids*, Vol. 1, May 1989, pp. 868–873.

[13]Koshigoe, S., Gutmark, E., Schadow, K. C., and Tubis, A., "Initial Development of Noncircular Jets Leading to Axis Switching," *AIAA Journal*, Vol. 27, April 1989, pp. 411–419.